A novel method for establishing typical daily profile of PM concentrations in underground railway stations

Valisoa M Rakotonirinjanahary, Suzanne Crumeyrolle, Mateusz Bogdan, Benjamin Hanoune

Indoor Environments 1 (2024) 100040

Contents lists available at ScienceDirect

Indoor Environments

journal homepage: www.sciencedirect.com/journal/indoor-environments

A novel method for establishing typical daily profile of PM concentrations in underground railway stations

Valisoa M. Rakotonirinjanahary[a,d,*], Suzanne Crumeyrolle[b], Mateusz Bogdan[c], Benjamin Hanoune[a]

[a] Univ. Lille, CNRS, UMR 8522 – PC2A – Physicochimie des Processus de Combustion et de l'Atmosphère, Lille F-59000, France
[b] Univ. Lille, CNRS, UMR 8518 – LOA – Laboratoire d'Optique Atmosphérique, Lille F-59000, France
[c] AREP L'hypercube, 16 avenue d'Ivry, Paris 75013, France
[d] SNCF Holding, 2 Place aux Etoiles, Saint-Denis 93210, France

ARTICLE INFO

Keywords:
Indoor air quality
Underground railway stations
PM concentrations
Daily profile
Temporal evolution

ABSTRACT

The air quality in underground railway stations (URS) poses a significant public health concern due to extremely high concentrations of particulate matter: PM_{10} and $PM_{2.5}$. Indeed, PM sources are strong and numerous, such as train braking and tunnel effect and URS are often confined spaces with low air change rates. Despite multiple PM measurements within URS, the variability of those concentrations from stations to stations is still poorly understood. We present here a methodology for establishing a daily profile of particle mass concentrations, based on a 5-year long measurement series in a Parisian URS. This approach incorporates an extensive data cleaning process based on the identification of URS operation periods and physically inconsistent or mathematically aberrant data, together with a linear regression model. This methodology delivers three usable outcomes: a typical profile for weekdays, a typical profile for weekends, and a PM concentration Daily Amplitude Coefficient (DAC) for the considered period. The DAC is a daily metric of the pollution levels, that enables the analysis of temporal trends and facilitates the comparison with other data with other acquisition frequency. The methodology developed here in a specific URS for PM_{10} measurements can be easily applied to different particle size fractions or to other measured parameters exhibiting a daily profile. Weekdays PM_{10} concentrations exhibit two distinct peaks corresponding to morning and evening rush hours, with an average daytime concentration of 193 $\mu g/m^3$. These peaks are delayed by ~1 hour compared to the train traffic. Weekends show consistently lower PM levels with no observable peaks, averaging 157 $\mu g/m^3$ during the day. Our analysis reveals the long-term temporal evolution of PM concentration within the URS, highlighting seasonal patterns with higher PM_{10} concentrations observed in summer (up to 400 $\mu g/m^3$) and lower values in winter (down to 250 $\mu g/m^3$). This indoor seasonal evolution is not correlated with the outdoor temporal evolution, showing higher concentrations during the winter. Furthermore, our results show that the optimal period (DAC ~ 1) for conducting experiments to obtain reliable profiles is during the spring months (April, May, June).

1. Introduction

Currently, trains represent the most widely utilized means of transportation, increasingly establishing themselves as indispensable components of daily commutes within major urban centers. The emphasis on air quality within trains and URS has grown significantly due to inherent factors like confined spaces, limited ventilation with high passenger number. Numerous investigations have shown that PM concentrations within URS consistently and largely exceed the air quality guidelines set by the World Health Organization [1], which stipulate daily outdoor thresholds of 45 and 15 $\mu g/m^3$ for PM_{10} (particles with an aerodynamic diameter up to 10 µm) and $PM_{2.5}$ (particles with an aerodynamic diameter up to 2.5 µm), respectively. Indeed, extremely high PM concentrations are observed in platforms areas. PM_{10} levels can reach up to 440 $\mu g/m^3$ in Nanjing, China [2], and as low as 51 $\mu g/m^3$ in Taipei, Taiwan [3]. For $PM_{2.5}$, concentrations vary from 18 $\mu g/m^3$ in Vancouver, Canada [4], to 195 $\mu g/m^3$ in Athens, Greece [5]. This variability is also noted in cities such as Stockholm, Sweden (204 $\mu g/m^3$ for PM_{10} and 102 $\mu g/m^3$ for $PM_{2.5}$) [6], and Los Angeles, USA (78 $\mu g/m^3$ for PM_{10} and 57 $\mu g/m^3$ for $PM_{2.5}$) [7]. A comprehensive list of PM

* Corresponding author at: Univ. Lille, CNRS, UMR 8522 – PC2A – Physicochimie des Processus de Combustion et de l'Atmosphère, Lille F-59000, France
E-mail address: miadanavalisoa.rakotonirinjanahary@univ-lille.fr (V.M. Rakotonirinjanahary).

https://doi.org/10.1016/j.indenv.2024.100040
Received 24 May 2024; Received in revised form 26 July 2024; Accepted 7 August 2024

concentrations in subway metro station platforms worldwide is provided by Passi et al. [8]. Additionally, elevated PM concentrations are also prevalent in the interior of trains, as observed in research carried out in Prague, Czech Republic (126 μg/m^3 for PM_{10}) [9], Seoul, Korea (142 μg/m^3 for PM_{10}) [10], or Lisbon, Portugal (80 μg/m^3 and 30 μg/m^3 for PM_{10} and $PM_{2.5}$) [11]. Moreover, the particle mass concentrations (PM_{10} and $PM_{2.5}$) within underground railway stations are several times higher than those in typical urban outdoor air. For instance, Raut et al. [12] reported that the average daytime PM_{10} and $PM_{2.5}$ concentrations of Paris URS were about 5–30 times higher than PM observed outdoor. Similarly, Carteni et al. [13] found that PM concentrations in Naples URS were 2–14 than those outdoors, and Smith et al. [14] observed the PM levels in London URS were approximately three times higher than those in the surrounding outdoor areas.

While passengers spend only brief periods (on average 7 minutes) [15] within these stations, even short-term exposure to heightened levels of air pollutants can lead to various adverse health consequences affecting the cardiovascular system, such as myocardial infarction and cardiac failure [16–18], as well as the respiratory system, with conditions including arrhythmia, deep vein thrombosis, stroke, wheeze, asthma, bronchiolitis, and other respiratory infections [19–23]. Furthermore, recent publications have connected this exposure to health issues like type 2 diabetes [24], dementia [25], and cognitive function decline [26,27]. In addition to its role as an air pollutant, PM can serve as a carrier for toxic and harmful substances such as bacteria or viruses, as evidenced by the global COVID-19 pandemic [28], thereby presenting a significant health risk to exposed individuals. Consequently, addressing air quality concerns within URS emerges as a critical imperative for public health.

According to Fortain [29], we can distinguish different sources of particles in an URS. First, railway activity generates a large quantity of particles. They can have various origins: equipment wear (brakes, wheel/rail and pantograph/catenary friction, ballast) primarily producing metallic particles, network wear (wear of walls, seats, and especially floor coverings), and nightly maintenance work specific to railway activity [30]. Moreover, the mechanism of the passenger-flow source is the resuspension of airborne particles by passenger movements [31]. Finally, as station openings and ventilation systems are often located close to traffic routes, they serve as pathways for outside air to enter the station, thereby introducing pollutants into the URS.

Several studies, including those conducted by Barmparesos et al. [5] and Kam et al. [7], have put forth measurements of PM concentrations in URS. Findings show that there are significant variations from one URS to another, and from one day to another within a given URS. Nevertheless, Raut et al. [12], Birenzvige et al. [32], Querol et al. [33], and Walther and Bogdan [34] have demonstrated different diurnal cycle patterns between weekdays and weekend periods. On weekdays, a regular bimodal pattern of train traffic is observed with two rush periods (morning and late afternoon) and minimum levels during the night leading to the similar PM concentration daily pattern. During weekends, the concentrations remain relatively constant during daytime with lower levels in comparison to weekdays. Furthermore, they found that the daily PM concentration pattern and the timing of the diurnal cycle are remarkably consistent from one day to the next, despite observing day-to-day fluctuations in PM concentration levels.

According to the actual knowledge of the authors, no study has addressed the establishment of a baseline daily profile of particle concentration reflecting the weekday and weekend patterns. The present work introduces a clear methodology to provide a typical daily profile of particle concentrations within a URS based on long term measurements performed in different URS, aiming to surpass simple profile averaging.

2. Experimental section

This study relies on the existence of a unique dataset spanning over five years, recorded at quarter-hourly intervals. This extensive and detailed dataset allows for precise analysis, setting the foundation for the insights presented in our study.

Table 1
URS characteristics.

	Characteristics
RER line	Line C
Mechanical ventilation system	No
Platform depth	~10 m below ground
Operation start	1854
Ballast	Yes
Passengers number (#/year)	982 800
Tracks	2
Platform	1
Length	250 m
Platform screen door	No
Train type	Z5600, Z8800, Z20500, Z20900

Note: RER line C is one of the lines of the Réseau Express Régional (RER) in Paris, which serves the Paris metropolitan area and its suburbs.

2.1. Measurement site

This study is based on experimental data in one Parisian URS (Table 1) within the SNCF network. This specific station has been selected for the development of the methodology because it is one of the three URS in the SNCF network that has been equipped with instrumentation (**Section 2.2**) for continuous data measurement since April 2018. This extended period of data collection allows a comprehensive analysis of air quality trends over time. 24 other stations were equipped for shorter periods ranging from one to three weeks. This specific station is also among the SNCF URS with the highest PM concentrations. Finally, this station has been the subject of experimental interventions, including the installation of filtration systems in 2019 and 2020. The methodology developed within this study will eventually allow to assess the effectiveness of these filtration systems.

No assumption is made that this station is representative of the URS within the Paris urban train stations network. This will be examined in a future global analysis of all PM levels inside the 27 stations.

The schematic plan of the URS is shown on the Fig. 1 with the main characteristics described in Table 1. The station consists of two train tracks (Northbound, from left to right; Southbound, from right to left; and a central platform) and the length of the central platform is approximately 250 m.

2.2. Instrumentation

The particle measurements were conducted using two TEOM FDMS 1405 F particle analyzers, to measure PM_{10} and $PM_{2.5}$ according to standard NF EN 12341 by FDMS (measurement by micro-balance, considering the volatile fraction of particles). These analyzers utilize a tapered element oscillating microbalance (TEOM) coupled with a filter dynamic measurement system (FDMS), ensuring high short-term precision (mean concentration values at 15-minute intervals). One of the two analyzers is equipped with a PM_{10} US EPA sampling head, while the other includes a PM_{10} US EPA sampling head in addition to a Sharp Cut Cyclone (SCC) for $PM_{2.5}$ sampling. Both instruments were positioned in the middle of the platform (Fig. 1) and were sampling at 2.2 m above the platform floor.

In addition to the TEOMs, a TSI Q-TRAK device was installed adjacent to them, enabling the measurement of temperature, relative humidity, and CO_2 concentrations. Similar to the PM concentrations, measurements of these parameters were taken at a quarter hourly time step.

AIRPARIF (https://www.airparif.asso.fr/, last access: May 16, 2024), a French Air Quality Monitoring Association in the Île-de-France region, conducted the data collection since April 2018. Regular

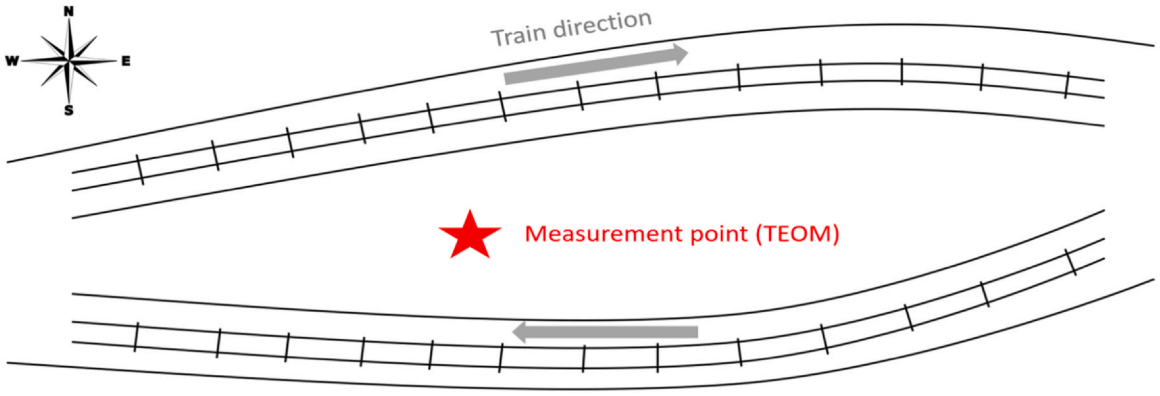

Fig. 1. Plan of the considered URS.

verification, maintenance, and calibration operations ensure that the collected data are of satisfactory precision, accuracy, completeness, comparability, and representativeness. A validation process by qualified personnel consists of two mandatory steps: a technical validation (conducted daily), and an environmental validation (conducted on a weekly basis). Invalidation may result from technical issues with the analyzer, external events (such as power outages) rendering the data unrepresentative, etc.

Data exploitation is based on validated readings. A data point is considered valid if at least 75 % of its constituent elements are valid. For instance, an hourly average is computable if at least 75 % of the 15-minute data points are valid, whether consecutive or not within the hour [35].

2.3. Dataset

The dataset for the considered URS covers the period from April 2018 to the present day. For the purposes of this study, we focus on the data spanning from April 2018 to December 2022. In this study, we focus on PM_{10} fraction, but similar work has been performed on $PM_{2.5}$ fraction, giving similar results.

Fig. 2 illustrates the timeseries of PM_{10} concentrations at a quarter hourly time steps within the specified URS, highlighting notable periods that have influenced the dynamics of the RER C line, including strikes (green band), COVID-19 lockdowns (orange band), summer works (blue band), and particle filtration experiment periods (grey band) (Table S1, supplemental material). The descriptive statistics for the PM_{10}, $PM_{2.5}$, and comfort parameters (CO_2, relative humidity, temperature) are presented in Table 2.

3. Establishment of typical daily profile PM concentration

Upon examining one week of data, Fig. 3 clearly illustrates the diurnal cycle patterns of PM_{10} between weekdays and weekend periods in the URS as discussed by Raut et al. [12] and Walther and Bogdan [34]. Throughout Monday to Friday (grey area), the daily PM_{10} concentration during daytime follows a similar trend and decreases during the weekend (green area). During weekdays, two peaks of PM_{10} concentration occurring generally during rush periods (in average $\sim 300\ \mu g/m^3$ against $\sim 320\ \mu g/m^3$ [12]) are observed followed by reaching its minimum levels ($10\ \mu g/m^3$) during the night after traffic stop. The PM_{10} concentration begins to increase at 5:30 am corresponding to the train operation start, reaching its first peak at 10:00 am. It then decreases at 01:00 pm (around $250\ \mu g/m^3$), followed by a subsequent increase, reaching its second peak at 07:00 pm, and finally decreases during the night. During weekends, the concentrations remain almost constant during daytime (in average $\sim 150\ \mu g/m^3$, against $\sim 120\ \mu g/m^3$ [12]).

Moreover, the one-week dataset displayed on Fig. 3 reveals deeper insights, as previously highlighted [12,34]. For instance, the overnight peaks circled in blue are attributed to nocturnal work within the station and the passage of diesel trains, while the daytime peaks circled in red remain unexplained.

Typically, discussions about the typical profile of PM concentration involve calculating only the average, often overlooking the fact that some profiles deviate from this pattern. This oversight can lead to an inaccurate typical profile, especially when working with limited datasets. In this section, we provide a concise overview of the rigorous methodology used to establish the typical profile of PM concentration,

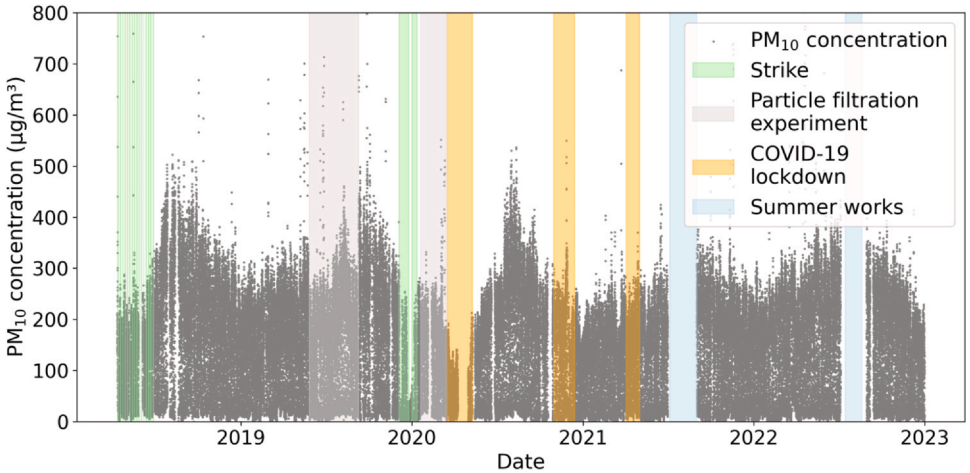

Fig. 2. Timeseries of PM10 concentrations (2018–2022). Shaded area corresponds to notable periods: strikes (green bands), COVID-19 lockdowns (orange bands), summer works (blue bands) and particle filtration experiments (grey bands).

Table 2
Summary statistics of collected data during the considered period.

Variables	Data points	Unit	Range (min, max)	Range (25th, 75th percentile)	Mean	SD
PM_{10}	141 428	$\mu g/m^3$	(0.1, 4492.9)	(60.1, 214.8)	146.6	102.2
$PM_{2.5}$	138 741	$\mu g/m^3$	(0.1, 2684.2)	(29, 84.3)	60.2	42.2
CO_2	143 817	ppm	(351, 1456)	(436.3, 526)	494.9	83.1
RH	142 767	%	(26.6, 90.4)	(51, 66)	58.5	10.3
T	142 691	°C	(8.6, 31.2)	(14.4, 22.9)	18.3	4.9

Note: SD = standard deviation; RH = relative humidity; T = temperature

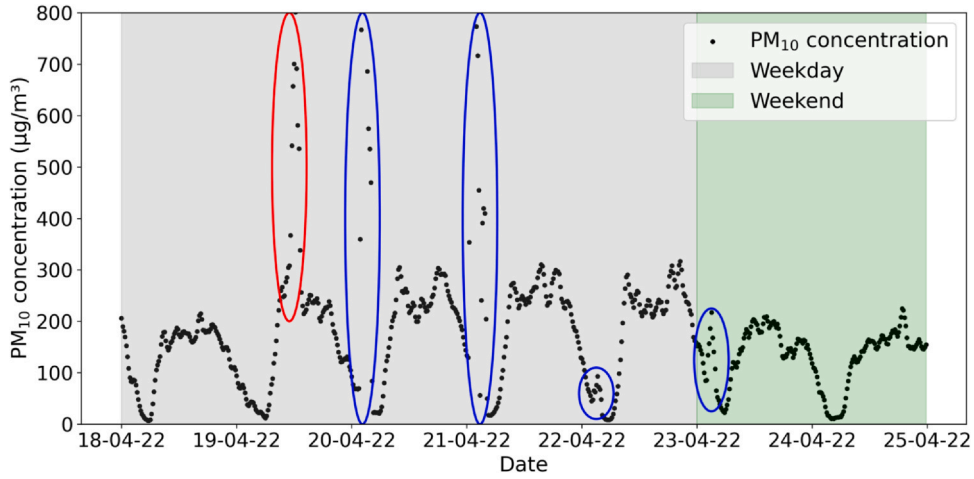

Fig. 3. PM_{10} concentration time profile for one week (18/04/2022–25/04/2022) inside the considered URS.

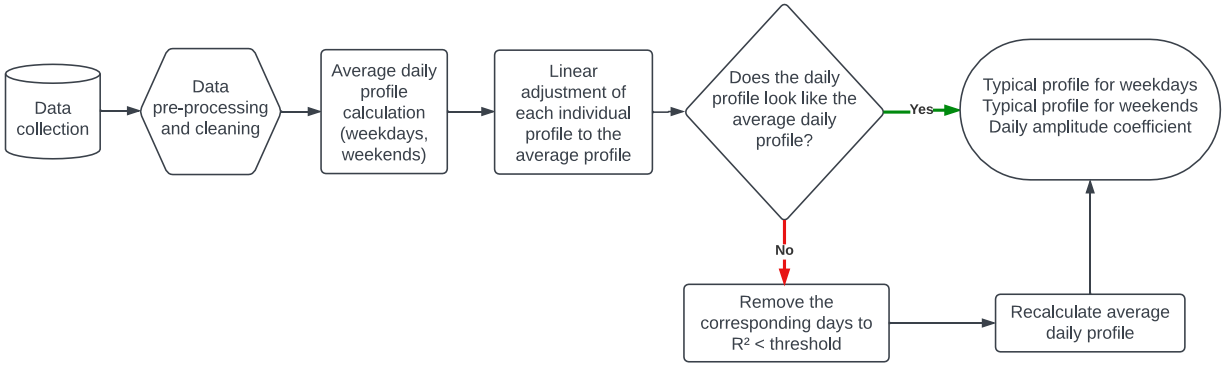

Fig. 4. Flowchart for the establishment of typical profile PM concentration.

visually presented on the flowchart in Fig. 4. Weekdays and weekends are treated separately due to different train schedules during these two periods, leading to different PM_{10} profiles (Fig. 3).

The methodology involves three main steps (Fig. 4): data pre-processing and cleaning (**Section 3.1**), profile fitting (**Section 3.2**), and statistical profile exclusion (**Section 3.3**). Thus, this methodology yields three usable outputs: a typical profile for weekdays, a typical profile for weekends, and a Daily Amplitude Coefficient (hereafter referred to as "DAC") associated with each daily profile within the considered period. The following subsections explain each step of our methodology in details.

3.1. Data preprocessing and cleaning

Dataset often presents gaps and noise, especially concerning PM concentration in URS. These issues may arise from missing values, outliers, and uncertainties in measurement, alongside exceptional events that could disrupt the data analysis process. Addressing these challenges is crucial as missing values and errors can greatly impact the accuracy of analytical techniques and the interpretation of the results. Consequently, the first step of our methodology involves data pre-processing, which encompasses the exclusion of notable periods and the identification and removal of outliers from our initial dataset.

Between April 2018 and December 2022, normal train operations of the considered URS have been disrupted several times (Fig. 2, Table S1 supplemental materials). During those periods, PM_{10} concentrations are not representative of URS regular functioning and normal concentration levels. Consequently, these periods were completely removed from our database. This step resulted in the removal of 21 % of the initial data (Table 3).

As previously noted, PM concentrations within URS tend to be higher than those outdoors. This circumstance results in a rapid degradation of instrument response over time. Moreover, the measurements of both particle fractions are carried out by two distinct TEOMs. Consequently, in our database, instances occur where $PM_{2.5}$ concentrations are higher than those of the PM_{10} fraction, especially during early morning when the concentrations are low (down to 5 $\mu g/m^3$) due to the absence of train operations. Therefore, all data points corresponding to $PM_{2.5}$ larger than PM_{10} concentrations were excluded from the initial database. This step leads to the removal of 4 % invalidated data (Table 3).

Table 3
Summary of data cleaning steps and proportion of data points removed.

Data cleaning steps	Proportion of data points removed from initial database
Strikes	4 %
COVID – 19 lockdowns	7 %
Summer works	1 %
Particle depollution experiment	9 %
Invalidated data	4 %
Outliers	1 %
Total	26 %

Outlined in Fig. 3, the dataset highlights outliers during nighttime hours (blue circle), accounting for 0.25 % of the initial database, and during daytime (red circle), accounting for 0.75 %. To address these outliers, various statistical-based approaches were tested, including descriptive statistics (histogram, boxplot: Interquartile Range), statistical tests (Z score), proximity-based methods (K-Nearest neighbor, Local Outlier Factor), and tree-based approaches (Isolation Forest). Among these, Isolation Forest proved to be the most satisfactory solution for our dataset. It successfully detects outliers not only during daytime (as shown by the peaks circled in red in Fig. 3) but also during nighttime (as evidenced by the peaks circled in blue in Fig. 3). In this study, we employed this approach, an unsupervised machine learning algorithm pioneered by Liu et al. [36]. This algorithm specializes in identifying anomalies within a dataset, specifically outliers that significantly differ from most of other data points. We used a dataset with specific characteristics: size of $n = 141428$ data points, dimensionality of $d = 1$, and contamination rate of 0.004. The contamination rate was set based on our data volume, as it reflects the proportion of data points expected to be anomalies. This step leads to the removal of 1 % of outliers (Table 3).

One can also note that holidays may lead to a reduced train and traveler frequency within the considered URS. To understand the impact of those breaks in comparison to normal operation, we selected the month when holidays occur (winter – February, spring – April, summer – July, fall – October breaks) across the entire period. During the months, we segregated the observed PM_{10} concentrations into two categories: those recorded during the holidays and those during the remainder of the month. Comparing the PM_{10} levels between these two periods revealed almost no difference, with an average variation of about 5 %, except for summer due to insufficient July data availability. Therefore, holiday periods are considered as suitable for retention in the dataset. To make this determination, we referred to the data shown in the supplementary material section (Figure S1), which compares periods with and without breaks at the considered URS.

Table 3 presents a comprehensive overview of the data cleaning result. It is important to note that the majority of removed data points are attributed to station operation, accounting for approximately 21 % of the initial database, while only 5 % are related to raw data. Overall, 26 % (36 089) of data points have been excluded from the initial database, leading our clean database with 105 339 data points of PM_{10}.

3.2. Profile fitting

In this section, our goal is to go beyond simple profile averaging. Indeed, it is imperative to refine the dataset by excluding profiles that are less representative. This entails aligning individual daily profiles with the overall daily average profile and removing those that significantly deviate from it. In essence, this step involves the identification of individual daily profiles that do not conform to the average daily profile.

An initial average daily profile (red dotted line for weekdays, Fig. 5a) is calculated, point by point at a quarterly hourly time step, using all daily profiles remaining after the data preprocessing and cleaning (**Section 3.1**).

Each individual day is then compared to this initial average daily profile. For this comparison, we perform a simple linear regression constrained to zero. This choice of constraint is based on the fact that all data points fall within a range of higher concentration, approximately around 200 µg/m^3 (Fig. 5). This model helps to establish the relationship between each time step (quarterly time step) of the individual profile (the dependent variable) to the corresponding time step of the average daily profile (the independent variable). The resulting slope, referred to hereafter as the daily amplitude coefficient (DAC), is calculated over 96 (4*24) data points for each individual profile. This DAC quantifies the amplitude of an individual profile relative to the average daily profile. When DAC is greater than 1 (lower than 1), the concentration during the specific day is higher (lower) than the average PM_{10} concentration profile.

As an example, Fig. 5b illustrates the linear regression model applied to the profile on November 10, 2022. The resulting DAC for this specific day is calculated to be 1.33, indicating that the amplitude of the profile on that day exceeds the initial average daily profile. Furthermore, the high coefficient of determination ($R^2 = 0.96$) for this individual day suggests a strong fit to the initial average daily profile.

3.3. Statistical profile exclusion

Once each individual daily profile was adjusted to the initial average daily profile, we employed a filtering concept based on R^2 to exclude profiles that deviated significantly from the average. R^2 measures the agreement between each individual daily profile and the average daily profile, with a maximum value of 1 indicating a perfect match.

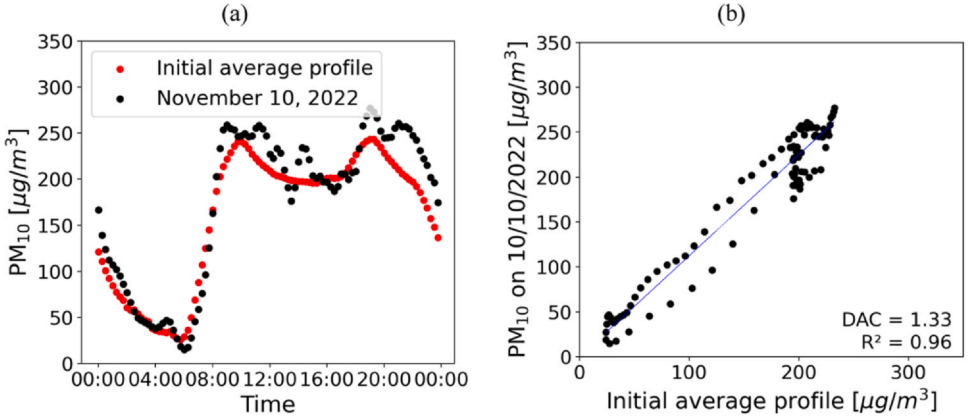

Fig. 5. (a) Profiles comparison: initial average profile (red dotted line) and the profile on November 10, 2022 (black dotted line), (b) Linear regression model, based on each PM measurements of the daily profile, for PM_{10} average profile and PM_{10} profile on that day.

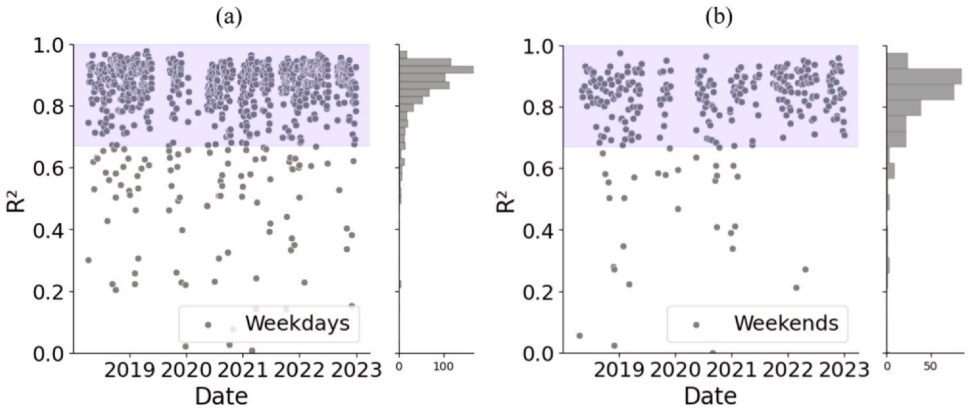

Fig. 6. Temporal variation of the daily goodness of fit R^2 for (a) weekdays and (b) weekends over the considered period. The joint plots along margins show its distribution.

In this study, individual daily profiles with $R^2 \leq 0.67$ were excluded, for both weekdays (Fig. 6a) and weekends (Fig. 6b), from the clean database. This threshold of 0.67 was chosen based on the distribution of R^2 values represented by the histogram on the right of each figure, to ensure that daily profiles closely match the average daily profile (Fig. 6). Through extensive testing, we determined that profiles with an R^2 below this value did not sufficiently align with the initial average profile. As with the DAC, this process was systematically repeated for each day within the study period. In the end of this process, 88 % (72 576 data points) and 90 % (25 632 data points) of profiles were retained (blue band, Fig. 6a and b) for weekdays and weekends, respectively, and two new average daily profiles were recalculated, representing the ultimate typical daily profiles (weekdays and weekends), as outlined in the flowchart in Fig. 4.

4. Results and discussions

4.1. Daily profiles

As previously mentioned, the aim of this study is to establish a clean daily profile. By meticulously applying all steps outlined in our methodology (**Section 3**), Fig. 7(a and b for weekdays and weekends, respectively) illustrates our reference daily profile (blue shaded areas represent one standard deviation), alongside initial average profile (red dotted line).

Weekdays and weekends exhibit distinct patterns, as discussed by Raut et al. [12] and Walther and Bogdan [34]. On weekdays, two peaks are observed during the morning (10:00 am) and evening (07:00 pm) rush hours, with the maximum amplitude of the profile reaching around 250 µg/m^3 for the considered URS. The average daytime PM concentration on weekdays is 193 µg/m^3. On the weekend, lower PM concentrations are observed, with an average daytime PM concentration of 157 µg/m^3 and no observable peaks, remaining almost constant during daytime (around 170 µg/m^3). Indeed, train operation differs between these two periods of the week, with trains operating from 05:00 am until 11:30 pm on weekdays and from 05:00 am until 01:00 am the following day on weekends. Moreover, during weekdays, trains run approximately every 8 minutes during rush hour and every 15 minutes outside of peak times explaining the two observed peaks during weekdays. While, during weekends, the frequency remains all daylong to approximately every 1 per 15 minutes, leading to alterations in the dynamics of the URS.

At the start of train operations (05:00 am), there is a one-hour delay before PM_{10} concentrations begin to rise (06:00 am) for both weekdays and weekends. This observation aligns with the findings of Raut et al. [12] and Birenzvige et al. [32], who noted that concentrations closely track traffic intensity but with a delay of approximately an hour. Indeed, their findings emphasize that this delay is primarily attributed to the influence of particulate dispersion by resuspension caused by traffic intensity and an increasing number of passengers.

Regarding the difference between the final reference profile and the initial average profile, we computed the Mean Absolute Error (MAE). The MAE values were 2.9 µg/m^3 for weekdays and 3.7 µg/m^3 for weekends. These results underscore the varying degrees of divergence between the initial average and reference daily profiles. The smaller difference between these profiles (weekdays and weekends) can be attributed to the volume of data.

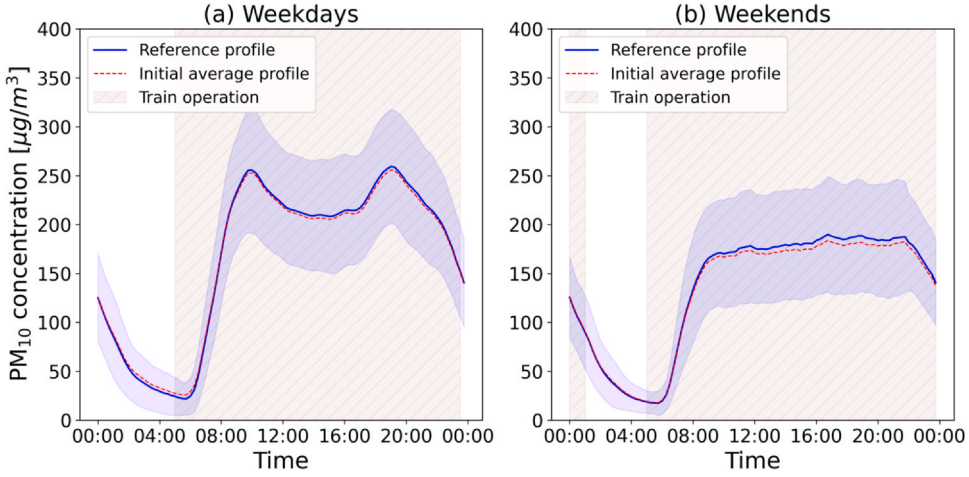

Fig. 7. Comparison between the reference profile (blue line) and the initial average profile (red dashed line) for (a) weekdays, and (b) weekends. Blue shaded areas represent one standard deviation (σ = 1).

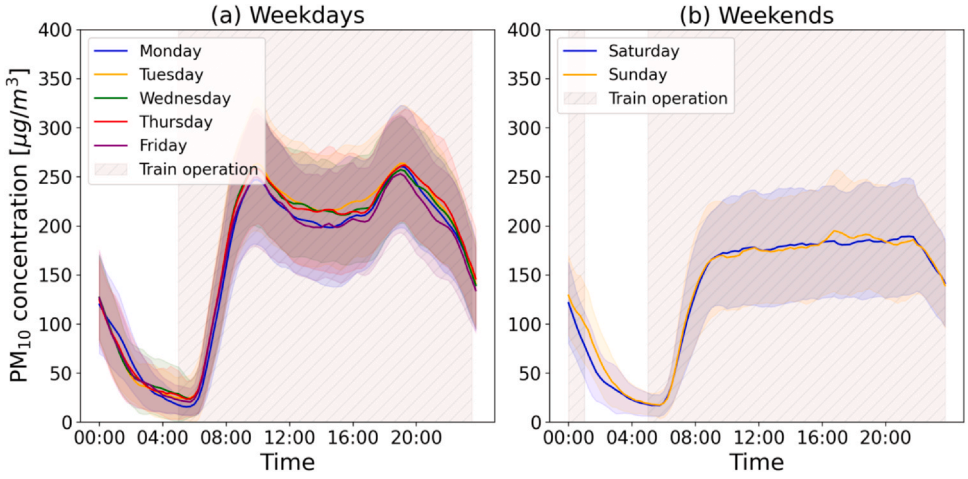

Fig. 8. Typical profiles at the considered URS for (a) weekdays and (b) weekends. Hatched shaded area indicates the train operation. Shaded areas represent one standard deviation (σ = 1).

Examining the day-of-week profiles shown in Fig. 8, it is notable that the profiles for Monday through Friday exhibit significant similarities, as do those for Saturday and Sunday. All profiles depicted in Fig. 8(a) and (b) fall within the shaded region representing one standard deviation. Moreover, the typical profiles for Monday to Friday share similarities due to consistent train operations from 05:00–23:00 (hatched shaded area, Fig. 8a), as do those for Saturday and Sunday, operating from 05:00–01:00 (hatched shaded area, Fig. 8b). Across all these profiles, concentrations decrease from the end of service until reaching approximately 10 μg/m^3 in the morning around 05:00 am, clearly indicating that particle presence is strongly associated with station operation. Indeed, the MAE between PM_{10} final profiles observed on Tuesdays and Fridays, representing the highest and lowest concentration profiles respectively, is only 10 μg/m^3. Similarly, the MAE between PM_{10} final profiles observed on Saturdays and Sundays on weekends is merely 4 μg/m^3. These observations attest that our reference profile is sufficiently robust to serve as a baseline reference for assessing air quality in URS. It is worth mentioning that the concentrations values observed are consistent with the published concentrations of particles on the platforms of underground train or subway stations in various cities, as given in the global list compiled by Passi et al. [8] in 2021.

4.2. Monthly analysis

In this section, we will initially verify whether the profile remains consistent to our reference profile (blue line, Fig. 7) across all months. Subsequently, we will move into the analysis of the monthly variations of the reference profile. Fig. 9 illustrates the profile calculated for each month over the entire period. These typical daily profiles for each month were derived by averaging all the data observed during the specific month of the full dataset, for weekdays and weekends. PM concentration levels notably increase during the months of July, August, September, and October for both weekdays and weekends, followed by a decrease during the months of December, January, February, and March.

During weekdays, the absolute maximum PM concentration level (~320 μg/m^3) is observed during the morning peak (10:00 am) in August, while the daytime minimum (~175 μg/m^3) occurs between the two peaks of the day (02:00 pm) in January. On weekends, however, the PM concentration remains relatively constant during daytime, with pronounced levels reaching 275 μg/m^3 and 250 μg/m^3 for August and July, respectively.

While the amplitude varies between each period due to seasonal variation, our analysis reveals that the reference profile pattern generally remains consistent throughout the months. Table 4 presents the statistical analysis of the DAC during each month (median value, 25th percentile, and the 75th percentile), as well as for the full period (2018–2022), so as to check for the stability of the daily profiles on the long term. Blanks corresponds to instances where no data were available, or data were removed during preprocessing and cleaning (**Section 3.1**), or excluded from statistical profile exclusion criteria (**Section 3.3**) or not representative due to having less than 50 % of the data points available.

It is worth noting that during August and July, the concavity between the two peaks of the day (10:00 am to 07:00 pm) on weekdays is less pronounced. This observation can be tentatively explained by changes in passenger routines during these months or may be artificially caused by missing data points. Specifically, data for July and August were only available in 2018 and 2019 with more than 50 % of the data points available (Table 4). Moreover, the reduced number of data points, which consequently leads to increased variability, may also explain the high amplitude observed during weekends (grey and cyan curves, Fig. 9b).

4.3. Long term evolution of PM concentration in the URS

Fig. 10 shows the original variation of quarter hourly PM_{10} concentration together with the DAC within the considered period. With access to a unique database covering approximately five years data, we can now quantify the impact of seasonality on PM_{10} concentrations. A relatively constant trend is observed throughout the observed period, with higher values during the summer (up to 400 μg/m^3) and lower values during winter (down to 250 μg/m^3). These findings are also evident from the temporal variation of DAC (blue dots, Fig. 10) and the monthly distribution of DAC (Fig. S3, supplemental material).

During summer, maximum DAC values are approximately 1.5, whereas during winter, these values drop to around 0.5. This suggests a discernible departure from the typical trend of PM concentration based on the season. The typical seasonal profile at the considered URS is illustrated in Fig. S2 (supplementary material).

Based on these findings, we can infer approximately a 1.5-fold difference between summer and winter, implying that knowledge of the typical profile of one season might enable us to approximate the profile of the other.

Based on Table 4, we followed a similar process for the PM_{10} outdoor data (as referenced in Table S2, supplemental material). The PM_{10} outdoor data were collected from the measurement station closest to the considered URS. Fig. 11 illustrates the radar plot of monthly distribution of the DAC mean value of PM_{10} within the considered URS

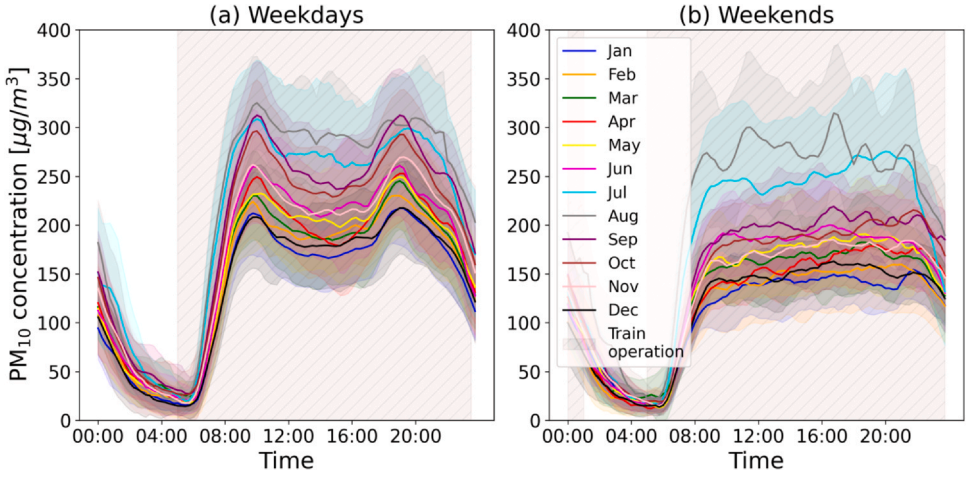

Fig. 9. Typical monthly profile for (a) weekdays and (b) weekends. Shaded areas represent one standard deviation (σ = 1).

Table 4
DAC averaged statistics for each month (median, 25th percentile, and 75th percentile).

DAC Median (25^{th} -75^{th} percentile)	2018	2019	2020	2021	2022	2018–2022
January	-	0.88 (0.84–0.99)	-	0.72 (0.69–0.79)	0.84 (0.80–0.90)	0.83 (0.74–0.89)
February	-	0.96 (0.87–1.08)	-	0.81 (0.72–0.89)	0.94 (0.87–0.98)	0.89 (0.80–0.96)
March	-	0.95 (0.87–1.06)	-	0.82 (0.74–0.93)	1.02 (0.94–1.15)	0.95 (0.82–1.06)
April	-	1.00 (0.94–1.09)	-	-	0.98 (0.90–1.05)	0.99 (0.93–1.08)
May	-	1.13 (0.90–1.18)	0.69 (0.62–0.81)	0.87 (0.76–0.91)	1.14 (1.07–1.26)	0.99 (0.81–1.16)
June	0.95 (0.86–0.99)	-	0.96 (0.89–1.13)	0.98 (0.84–1.04)	1.17 (1.09–1.30)	1.01 (0.90–1.17)
July	1.31 (1.14–1.61)	-	1.23 (1.00–1.48)	-	-	1.27 (1.07–1.51)
August	1.43 (1.32–1.55)	-	1.35 (1.26–1.50)	-	-	1.38 (1.31–1.54)
September	1.29 (1.18–1.40)	-	1.16 (1.06–1.26)	1.10 (1.05–1.15)	1.15 (1.09–1.21)	1.16 (1.09–1.26)
October	1.20 (1.11–1.29)	1.27 (1.20–1.43)	-	0.99 (0.96–1.06)	1.12 (1.03–1.21)	1.14 (1.02–1.27)
November	1.11 (0.96–1.23)	1.10 (1.04–1.19)	-	0.96 (0.86–1.01)	0.97 (0.91–1.03)	1.02 (0.92–1.11)
December	0.98 (0.97–1.06)	-	-	0.88 (0.81–0.95)	0.72 (0.66–0.78)	0.87 (0.74–0.98)

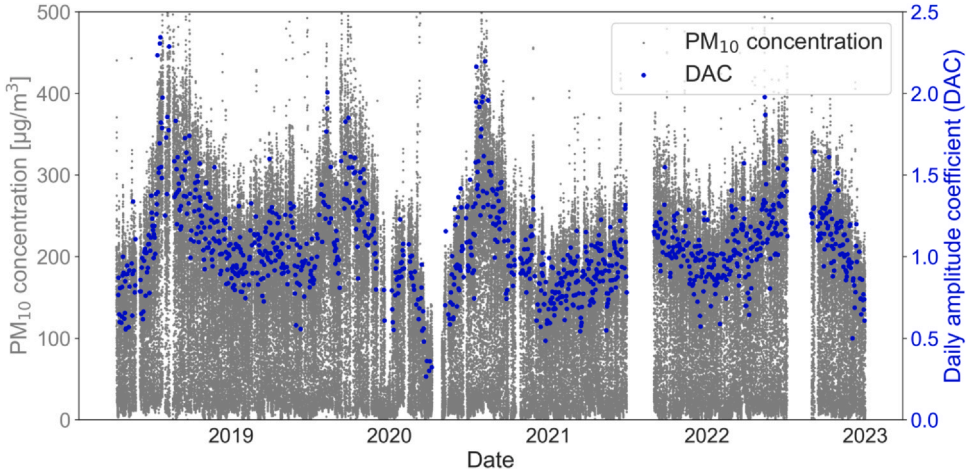

Fig. 10. Temporal evolution of DAC (blue dots) with original PM_{10} concentration (grey dots) (2018–2022).

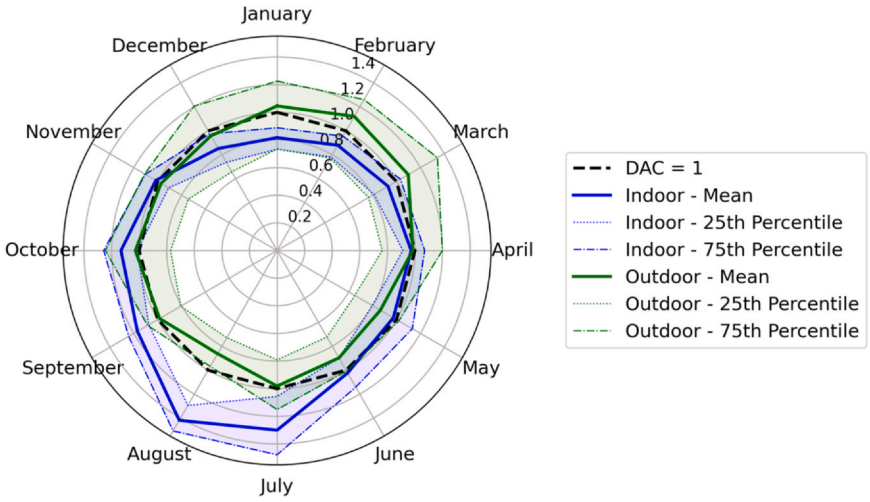

Fig. 11. Radar plot showing monthly distribution of the DAC mean value of PM_{10} within URS (blue) and the DAC mean value of outdoor PM_{10} (green) from the nearest station of the considered URS. The solid line represents the mean DAC value, the dotted line represents the 25th percentile, and the dash-dotted line represents the 75th percentile of DAC for the period 2018–2022.

(blue) for the entire period (2018–2022), alongside the DAC mean value of outdoor PM_{10} data (green) from the nearest measurement station for the same period. The black dashed line represents the reference level of PM_{10} ($\overline{DAC} = 1$). As already pointed out, PM_{10} concentrations (blue curves) are higher than the average level of the profile during the summer months (July, August, September), peaking in August ($\overline{DAC} \approx 1.3$), whereas they are lower in winter (December, January, February), with the lowest levels in January ($\overline{DAC} \approx 0.6$). This is not the case for the outdoor PM_{10} concentrations, exhibiting higher levels between January and March, peaking in February ($\overline{DAC} \approx 1.1$), and lower levels in the summer, reaching their minimum in August ($\overline{DAC} \approx 0.8$). For a detailed view of daily PM_{10} outdoor, see Fig. S4 (supplemental materials).

Furthermore, Fig. 11 shows that during the spring months (April, May, June), the mean DAC value of indoor PM_{10} consistently remains at 1. This suggests that the ideal period for conducting experiments within the considered URS to obtain a representative reference profile is during these months, as the indoor PM_{10} levels precisely match the reference profile level. It is worth to note that while this observation holds true for this specific URS, its applicability to other URSs requires further generalization.

These observations show that PM seasonal pattern inside a URS is entirely different from what is observed outdoors, as seen in the studies of H. Luo et al. [37] in China or Gokul et al. [38] in India, who stipulated that the amplitude of PM concentration in summer is smaller than that in winter. Additionally, contrary to the results of Kwon et al. [39] in Seoul, Korea or of Van Ryswyk et al. [4] in Montreal and Vancouver, Canada, these findings suggest higher concentrations during the warmer period.

Higher concentrations during the warmer period could be attributed, at least in part, to the train braking system and impacts of meteorological parameters. Walia et al. [40] stated that brake energy for the cast iron brake blocks for driving trailer during winter is lower as compared to summer.

5. Conclusions

In this paper, we presented a novel methodology for establishing a reference PM profile within an URS. In the first step, a standardized data preprocessing and cleaning process is performed (excluding specific operational periods, inconsistent data, and outliers). A pivotal component of this methodology is robust data cleaning, where we introduced an AI-based approach, to effectively detect outliers. Our results demonstrated the high accuracy of this tool, particularly in identifying daytime and nighttime outliers caused by station exploitation and nocturnal work within the station or the passage of diesel trains, respectively. Only 26 % of the initial database were removed, with approximately 21 % related to URS operation and only 5 % related to raw data.

In the second step, an iterative averaging method is implemented to obtain the reference profile over the entire considered period. It is mainly based on performing a simple yet effective linear regression model to identify individual daily profiles that deviate from the reference profile pattern and transform into a daily amplitude coefficient (DAC) for easier analysis. The DAC, as a daily metric of the pollution levels, enables the analysis of temporal trends, and facilitates the comparison with other data with other acquisition frequency. This model leverages the goodness of fit, allowing us to move beyond mere profile averaging and identify those profiles that do not align with the initial average profile. Profiles corresponding to R^2 values larger than 0.67 were selected from our dataset.

We observed two distinct peaks in PM concentration during weekdays, mainly occurring one hour after rush hours, with an average daytime PM concentration of 193 $\mu g/m^3$. In contrast, weekends showed lower PM concentration levels, averaging 157 $\mu g/m^3$, with no observable peaks. Additionally, this work relies on the utilization of a vast database spanning approximately five years, with data collected at quarter-hourly intervals. This extensive dataset allowed us to observe long-term trends, such as higher PM concentration values in summer and lower values in winter, with a noticeable stability in PM profile at both monthly and yearly scales. Furthermore, results suggest that the optimal period for conducting experiments within the considered URS to obtain a representative reference profile is during the spring months (April, May, June). Moreover, we found the indoor PM concentrations are decorrelated from the outdoor concentrations, highlighting different dynamics within the URS compared to the external environment. It should be emphasized that this versatile methodology, offering flexibility and applicability; should be applied to different particle classes at various URS. What sets this work apart is our departure from the traditional approach of solely averaging daily profiles to establish a reference at a given URS. Instead, our methodology rigorously filters out profiles that do not conform to the reference profile pattern. Our results highlight the effectiveness of our methodology in establishing a reference profile at the considered URS across various periods. The application of our methodology to other URS can be a valuable direction for future research or extension of the current methodology.

Declaration of Competing Interest

The authors declare that they have no known competing financial interests or personal relationships that could have appeared to influence the work reported in this paper

Acknowledgements

The authors greatly acknowledge SNCF for funding the PhD of Valisoa Rakotonirinjanahary (ANRT CIFRE PhD grant n°2021/0856, managed by the National Research Technology Agency). Authors are also grateful to AIRPARIF for conducting data collection. This research is part of the CaPPA project (Chemical and Physical Properties of the Atmosphere), funded by the French National Research Agency (ANR) through the PIA (Programme Investissement d'Avenir) with the contract ANR-11-LABX-005–001. Additionally, it is affiliated with the Institute of Multidisciplinary Research in Environmental Sciences (IRePSE Fed 4129) and the CPER ECRIN research project, funded by the French Ministry of Higher Education and Research, the Hauts-de-France Region, and the European Regional Development Fund.

Appendix A. Supporting information

Supplementary data associated with this article can be found in the online version at doi:10.1016/j.indenv.2024.100040.

References

[1] World Health Organization, WHO global air quality guidelines: particulate matter (PM2.5 and PM10), ozone, nitrogen dioxide, sulfur dioxide and carbon monoxide: executive summary, World Health Organization, 2021 accessed December 8, 2023〈https://iris.-who.int/handle/10665/345334〉.

[2] P. Mao, J. Li, L. Xiong, R. Wang, X. Wang, Y. Tan, H. Li, Characterization of Urban Subway Microenvironment Exposure—A Case of Nanjing in China, Int. J. Environ. Res. Public Health 16 (2019) 625, https://doi.org/10.3390/ijerph16040625.

[3] Y.-H. Cheng, Z.-S. Liu, J.-W. Yan, Comparisons of PM10, PM2.5, Particle Number, and CO2 Levels inside Metro Trains between Traveling in Underground Tunnels and on Elevated Tracks, Aerosol Air Qual. Res. 12 (2012) 879–891, https://doi.org/10.4209/aaqr.2012.05.0127.

[4] K. Van Ryswyk, A.T. Anastasopolos, G. Evans, L. Sun, K. Sabaliauskas, R. Kulka, L. Wallace, S. Weichenthal, Metro Commuter Exposures to Particulate Air Pollution and PM2.5-Associated Elements in Three Canadian Cities: The Urban Transportation Exposure Study, Environ. Sci. Technol. 51 (2017) 5713–5720, https://doi.org/10.1021/acs.est.6b05775.

[5] N. Barmparesos, V. D. Assimakopoulos, M.N. Assimakopoulos, E. Tsairidi, Particulate matter levels and comfort conditions in the trains and platforms of the Athens underground metro, AIMSES 3 (2016) 199–219, https://doi.org/10.3934/environsci.2016.2.199.

[6] M. Tu, U. Olofsson, PM levels on an underground metro platform: A study of the train, passenger flow, urban background, ventilation, and night maintenance effects, Atmos. Environ.: X 12 (2021) 100134, https://doi.org/10.1016/j.aeaoa.2021.100134.

[7] W. Kam, K. Cheung, N. Daher, C. Sioutas, Particulate matter (PM) concentrations in underground and ground-level rail systems of the Los Angeles Metro, Atmos. Environ. 45 (2011) 1506–1516, https://doi.org/10.1016/j.atmosenv.2010.12.049.

[8] A. Passi, S.M.S. Nagendra, M.P. Maiya, Characteristics of indoor air quality in underground metro stations: A critical review, Build. Environ. 198 (2021) 107907, https://doi.org/10.1016/j.buildenv.2021.107907.

[9] M. Braniš, The contribution of ambient sources to particulate pollution in spaces and trains of the Prague underground transport system, Atmos. Environ. 40 (2006) 348–356, https://doi.org/10.1016/j.atmosenv.2005.09.060.

[10] S.-B. Kwon, D. Park, Y. Cho, E.-Y. Park, Measurement of natural ventilation rate in Seoul metropolitan subway cabin, Indoor Built Environ. 19 (2010) 366–374, https://doi.org/10.1177/1420326X10367305.

[11] M.J. Ramos, A. Vasconcelos, M. Faria, Comparison of Particulate Matter Inhalation for Users of Different Transport Modes in Lisbon, Transp. Res. Procedia 10 (2015) 433–442, https://doi.org/10.1016/j.trpro.2015.09.093.

[12] J.-C. Raut, P. Chazette, A. Fortain, Link between aerosol optical, microphysical and chemical measurements in an underground railway station in Paris, Atmos. Environ. 43 (2009) 860–868, https://doi.org/10.1016/j.atmosenv.2008.10.038.

[13] A. Cartenì, F. Cascetta, S. Campana, Underground and ground-level particulate matter concentrations in an Italian metro system, Atmos. Environ. 101 (2015) 328–337, https://doi.org/10.1016/j.atmosenv.2014.11.030.

[14] J.D. Smith, B.M. Barratt, G.W. Fuller, F.J. Kelly, M. Loxham, E. Nicolosi, M. Priestman, A.H. Tremper, D.C. Green, PM2.5 on the London Underground, Environ. Int 134 (2020) 105188, https://doi.org/10.1016/j.envint.2019.105188.

[15] H. Marcus, Waiting experience at train stations, Journal of Medical Internet Research - J MED INTERNET RES (2011).

[16] R. Luo, H. Dai, Y. Zhang, P. Wang, Y. Zhou, J. Li, M. Zhou, L. Qiao, Y. Ma, S. Zhu, S. Hu, C. Huang, H. Shi, Association of short-term exposure to source-specific PM2.5 with the cardiovascular response during pregnancy in the Shanghai MCPC study, Sci. Total Environ. 775 (2021) 145725, https://doi.org/10.1016/j.scitotenv.2021.145725.

[17] M. Renzi, M. Stafoggia, P. Michelozzi, M. Davoli, F. Forastiere, A.G. Solimini, Short-term exposure to PM2.5 and risk of venous thromboembolism: A case-crossover study, Thromb. Res 190 (2020) 52–57, https://doi.org/10.1016/j.thromres.2020.03.008.

[18] L.H. Wyatt, A.M. Weaver, J. Moyer, J.D. Schwartz, Q. Di, D. Diaz-Sanchez, W.E. Cascio, C.K. Ward-Caviness, Short-term PM2.5 exposure and early-readmission risk: a retrospective cohort study in North Carolina heart failure patients, Am. Heart J. 248 (2022) 130–138, https://doi.org/10.1016/j.ahj.2022.02.015.

[19] T. Chen, F. Chen, K. Wang, X. Ma, X. Wei, W. Wang, P. Huang, D. Yang, Z. Xia, Z. Zhao, Acute respiratory response to individual particle exposure (PM1.0, PM2.5 and PM10) in the elderly with and without chronic respiratory diseases, Environ. Pollut. 271 (2021) 116329, https://doi.org/10.1016/j.envpol.2020.116329.

[20] R. Lei, F. Zhu, H. Cheng, J. Liu, C. Shen, C. Zhang, Y. Xu, C. Xiao, X. Li, J. Zhang, R. Ding, J. Cao, Short-term effect of PM2.5/O3 on non-accidental and respiratory deaths in highly polluted area of China, Atmos. Pollut. Res. 10 (2019) 1412–1419, https://doi.org/10.1016/j.apr.2019.03.013.

[21] L. Pini, J. Giordani, G. Gardini, C. Concoreggi, A. Pini, E. Perger, E. Vizzardi, D. Di Bona, C. Cappelli, M. Ciarfaglia, C. Tantucci, Emergency department admission and hospitalization for COPD exacerbation and particulate matter short-term exposure in Brescia, a highly polluted town in northern Italy, Respir. Med 179 (2021) 106334, https://doi.org/10.1016/j.rmed.2021.106334.

[22] B. Sun, J. Song, Y. Wang, J. Jiang, Z. An, J. Li, Y. Zhang, G. Wang, H. Li, N.E. Alexis, I. Jaspers, W. Wu, Associations of short-term PM2.5 exposures with nasal oxidative stress, inflammation and lung function impairment and modification by *GSTT1*-null genotype: A panel study of the retired adults, Environ. Pollut. 285 (2021) 117215, https://doi.org/10.1016/j.envpol.2021.117215.

[23] Y. Zhang, Z. Ding, Q. Xiang, W. Wang, L. Huang, F. Mao, Short-term effects of ambient PM1 and PM2.5 air pollution on hospital admission for respiratory diseases: Case-crossover evidence from Shenzhen, China, Int. J. Hyg. Environ. Health 224 (2020) 113418, https://doi.org/10.1016/j.ijheh.2019.11.001.

[24] C. Liu, G. Cao, J. Li, S. Lian, K. Zhao, Y. Zhong, J. Xu, Y. Chen, J. Bai, H. Feng, G. He, X. Dong, P. Yang, F. Zeng, Z. Lin, S. Zhu, X. Zhong, W. Ma, T. Liu, Effect of long-term exposure to PM2.5 on the risk of type 2 diabetes and arthritis in type 2 diabetes patients: Evidence from a national cohort in China, Environ. Int. 171 (2023) 107741, https://doi.org/10.1016/j.envint.2023.107741.

[25] D. Wood, D. Evangelopoulos, S. Beevers, N. Kitwiroon, K. Katsouyanni, Exposure to Ambient Air Pollution and the Incidence of Dementia in the Elderly of England: The ELSA Cohort, Int J. Environ. Res Public Health 19 (2022) 15889, https://doi.org/10.3390/ijerph192315889.

[26] E. Dimakakou, H.J. Johnston, G. Streftaris, J.W. Cherrie, Exposure to environmental and occupational particulate air pollution as a potential contributor to neurodegeneration and diabetes: a systematic review of epidemiological research, Int. J. Environ. Res. Public Health 15 (2018) 1704, https://doi.org/10.3390/ijerph15081704.

[27] J. Duchesne, L.-A. Gutierrez, I. Carrière, T. Mura, J. Chen, D. Vienneau, K. de Hoogh, C. Helmer, B. Jacquemin, C. Berr, M. Mortamais, Exposure to ambient air pollution and cognitive decline: Results of the prospective Three-City cohort study, Environ. Int. 161 (2022) 107118, https://doi.org/10.1016/j.envint.2022.107118.

[28] L. Chang, W.T. Chong, Y.H. Yau, T. Cui, X.R. Wang, F. Pei, Y.Q. Liu, S. Pan, An investigation of the PM2.5 concentrations and cumulative inhaled dose during subway commutes in Changchun, China, Int J. Environ. Sci. Technol. (Tehran) (2023) 1–14, https://doi.org/10.1007/s13762-023-04994-7.

[29] A. Fortain, Caractérisation des particules en gares souterraines, These de doctorat, La Rochelle, 2008. https://www.theses.fr/2008LAROS231 (accessed June 8, 2022).

[30] L. Chang, W.T. Chong, X. Wang, F. Pei, X. Zhang, T. Wang, C. Wang, S. Pan, Recent progress in research on PM2.5 in subways, Environ. Sci.: Process. Impacts 23 (2021) 642–663, https://doi.org/10.1039/D1EM00002K.

[31] C. Johansson, P.-Å. Johansson, Particulate matter in the underground of Stockholm, Atmos. Environ. 37 (2003) 3–9, https://doi.org/10.1016/S1352-2310(02)00833-6.

[32] A. Birenzvige, J. Eversole, M. Seaver, S. Francesconi, E. Valdes, H. Kulaga, Aerosol Characteristics in a Subway Environment, Aerosol Sci. Technol. 37 (2003) 210–220, https://doi.org/10.1080/02786820300941.

[33] X. Querol, T. Moreno, A. Karanasiou, C. Reche, A. Alastuey, M. Viana, O. Font, J. Gil, E. de Miguel, M. Capdevila, Variability of levels and composition of PM_{10} and $PM_{2.5}$ in the Barcelona metro system, Atmos. Chem. Phys. 12 (2012) 5055–5076, https://doi.org/10.5194/acp-12-5055-2012.

[34] E. Walther, M. Bogdan, A novel approach for the modelling of air quality dynamics in underground railway stations, Transp. Res. Part D: Transp. Environ. 56 (2017) 33–42, https://doi.org/10.1016/j.trd.2017.07.014.

[35] AIRPARIF, Mesures de la qualité de l'air intérieur sur les quais des gares souterraines franciliennes de la SNCF: Rapport final, AIRPARIF, 2020. https://www.airparif.asso.fr/etudes/2021/qualite-de-lair-interieur-quais-gares-sncf-rapport-final-2020 (accessed June 13, 2022).

[36] F.T. Liu, K.M. Ting, Z.-H. Zhou, Isolation Forest, 2008 Eighth IEEE Int. Conf. Data Min. (2008) 413–422, https://doi.org/10.1109/ICDM.2008.17.

[37] H. Luo, Y. Han, X. Cheng, C. Lu, Y. Wu, Spatiotemporal Variations in Particulate Matter and Air Quality over China: National, Regional and Urban Scales, Atmosphere 12 (2021) 43, https://doi.org/10.3390/atmos12010043.

[38] P.R. Gokul, A. Mathew, A. Bhosale, A.T. Nair, Spatio-temporal air quality analysis and PM2.5 prediction over Hyderabad City, India using artificial intelligence techniques, Ecol. Inform. 76 (2023) 102067, https://doi.org/10.1016/j.ecoinf.2023.102067.

[39] S.-B. Kwon, W. Jeong, D. Park, K.-T. Kim, K.H. Cho, A multivariate study for characterizing particulate matter (PM10, PM2.5, and PM1) in Seoul metropolitan subway stations, Korea, J. Hazard. Mater. 297 (2015) 295–303, https://doi.org/10.1016/j.jhazmat.2015.05.015.

[40] M.S. Walia, T. Vernersson, R. Lundén, F. Blennow, M. Meinel, Temperatures and wear at railway tread braking: Field experiments and simulations, Wear 440–441 (2019) 203086, https://doi.org/10.1016/j.wear.2019.203086.